



FULL LENGTH ARTICLE

Vitamin A deficiency suppresses CEACAM1 to impair colonic epithelial barrier function via downregulating microbial-derived short-chain fatty acids



Junyan Yan ^a, Lu Xiao ^{a,b}, Di Feng ^a, Baolin Chen ^a, Ting Yang ^a,
Bei Tong ^a, Ruifang Luo ^a, Yuting Wang ^{b,*}, Jie Chen ^{a,*}

^a Children Nutrition Research Center, Children's Hospital of Chongqing Medical University, Chongqing Key Laboratory of Child Nutrition and Health, Ministry of Education Key Laboratory of Child Development and Disorders, National Clinical Research Center for Child Health and Disorders, Chongqing 401122, China

^b Department of Gastroenterology, Children's Hospital of Chongqing Medical University, Chongqing 401122, China

Received 27 December 2022; received in revised form 8 March 2023; accepted 29 March 2023
Available online 24 May 2023

KEYWORDS

CEACAM1;
Colonic epithelial
barrier;
HDAC3;
Short-chain fatty
acids;
Vitamin A deficiency

Abstract Vitamin A (VA) plays an essential role in modulating both the gut microbiota and gut barrier function. Short-chain fatty acids (SCFAs), as metabolites of the gut microbiota, protect the physiological intestinal barrier; however, they are compromised when VA is deficient. Thus, there is an urgent need to understand how and which SCFAs modulate colonic epithelial barrier integrity in VA deficiency (VAD). Herein, compared with normal VA rats (VAN), at the beginning of pregnancy, we confirmed that the colonic desmosome junction was impaired in the VAD group, and the amounts of acetate, propionate, and butyrate declined because of the decreased abundance of SCFA-producing bacteria (*Romboutsia*, *Collinsella*, and *Allobaculum*). The differentially expressed genes correlated with the gut barrier and the histone deacetylase complex between the VAD and VAN groups were enriched by RNA sequencing. In the VAD group, the expression levels of colonic CEA cell adhesion molecule 1 (CEACAM1) were down-regulated, and the levels of histone deacetylase 1 (HDAC1) and HDAC3 were up-regulated. Intriguingly, the above changes in the VAD groups were rescued by VA supplementation in the early postnatal period. Further study indicated that in Caco-2 cells, butyrate treatment significantly repressed the enrichment of HDAC3 on the promoter of the *CEACAM1* gene to induce its expression. Our findings support that butyrate intervention can alleviate the

* Corresponding author.

E-mail addresses: charry_5678@163.com (Y. Wang), jchen010@hospital.cqmu.edu.cn (J. Chen).

Peer review under responsibility of Chongqing Medical University.

<https://doi.org/10.1016/j.gendis.2023.03.032>

2352-3042/© 2023 The Authors. Publishing services by Elsevier B.V. on behalf of KeAi Communications Co., Ltd. This is an open access article under the CC BY-NC-ND license (<http://creativecommons.org/licenses/by-nc-nd/4.0/>).

impairment of colonic barrier function caused by VAD, and timely postnatal VA intervention may reverse the damage caused by VAD on gut barrier integrity during pregnancy.

© 2023 The Authors. Publishing services by Elsevier B.V. on behalf of KeAi Communications Co., Ltd. This is an open access article under the CC BY-NC-ND license (<http://creativecommons.org/licenses/by-nc-nd/4.0/>).

Introduction

Vitamin A (VA) is critical for protecting the host from infections, enhancing epithelial barrier integrity, improving cognitive ability, and promoting immunity, in addition to promoting vision and growth. As reported by the latest study on “Global Burden of Vitamin A Deficiency in 204 Countries and Territories from 1990 to 2019”, the global incidence of vitamin A deficiency (VAD) has fallen by 44.19% from 1990 to 2019, and the global age-standardized incidence rate also shows a consistent downward trend. However, the burden of VAD remains high in regions with low socio-demographic indexes, and children younger than 5 years old are most affected by VAD.¹

VA is essential for protecting and maintaining the integrity and homeostasis of the gut barrier.² The gut barrier is composed of chemical, mechanical, immune, and microbial barriers. Previous studies have proven that VAD impairs the gut barrier by reducing the secretion of mucins,³ down-regulating tight junction protein levels,^{4,5} decreasing the intestinal immune cell response,^{6,7} and disturbing the gut microbiota structure.^{8,9} The imbalanced gut microbiome composition and its perturbed metabolites, such as short-chain fatty acids (SCFAs), secondary bile acids, indole, and tryptophan, have been proven to aggravate the impairment of the other three gut barriers.¹⁰ In our previous work, we found that the microbiota from children with VAN restored the epithelial barrier integrity in germ-free mice, while that from children with VAD did not.¹¹ This prompted us to further investigate the mechanism by which gut microbiome dysbiosis related to VAD modulates gut epithelial barrier integrity.

SCFAs, predominantly acetic acid, propionic acid, and butyric acid, are produced by gut microorganisms through fermenting dietary fiber or protein¹² and have been discovered to play a crucial role in protecting the gut barrier.¹³ As the preferred energy resource for colonic cells, the actions of SCFAs are related to triggering G protein-coupled receptors and inhibiting histone deacetylases (HDACs).^{14,15} Tian and coworkers found that VAD reduced the amount of acetic acid, propionic acid, and butyric acid in cecum contents. Therefore, we hypothesized that the dysregulated production of SCFAs resulting from a disorganized gut microbiota composition caused by VAD would participate in impairing gut epithelial barrier integrity. Meanwhile, we aimed to demonstrate whether this series of pathological processes could be rescued by postnatal vitamin A supplementation (VAS). To resolve the above questions, we first confirmed the reduction of SCFAs in the colons of offspring from the beginning of gestational VAD, and whether it could be rescued by postnatal VAS. Then, the combination of 16S rDNA gene sequencing of the gut microbiome in cecum contents and colon tissue

transcriptome sequencing was conducted in rats from the VAN (normal VA control), VAD, and VAS groups, to identify the specific downstream targets of SCFAs associated with gut barrier functions. Lastly, butyrate was used to stimulate Caco-2 cells *in vitro* to verify the specific epigenetic modulatory mechanisms. The present research provides a novel perspective to explore the mechanisms by which VAD impairs gut epithelial barrier integrity, and suggests a potential application to guide clinical practice in which SCFA impairment should be concerned when treating intestinal barrier dysfunction caused by VAD.

Methods

Animals, diets, and sample collection

Female Sprague–Dawley rats aged three weeks old were purchased from Chongqing Medical University and maintained in individually ventilated cages in the same rodent house with a controlled temperature of 22–24 °C and a 12-h light/12-h dark cycle in the Children’s Hospital of Chongqing Medical University Animal Care Centre. After adapting to the new environment for one week, the rats were randomly divided into the maternal VAN group ($n = 3$) and the maternal VAD group ($n = 6$). The rats in the maternal VAN group were fed a VAN diet with 6500 IU/kg VA, while the rats in the maternal VAD group were fed a VAD diet with 300 IU/kg VA for four weeks. Then, the retinol concentration was measured. The retinol concentration of the maternal VAN rats was $>1.05 \mu\text{mol/L}$, and that of maternal VAD rats was $<0.7 \mu\text{mol/L}$; therefore, they were mated with male rats. The pregnant rats in the maternal VAN and VAD groups were fed separately with a VAN or VAD diet until the pups were born. Next, three cages of the maternal VAD rats and their offspring were randomly selected as the VAS group, whose diet was changed to a VAN diet, and the pups received vitamin A supplementation at 83.3 IU/d for seven days by oral gavage. The other three cages comprised the VAD group and were fed a VAD diet. The maternal VAN rats and their pups were still fed a VAN diet and were termed the VAN group. When the offspring were three weeks old, their blood was collected, and the cecum contents, colonic contents, and colon tissue were obtained and snap-frozen with liquid nitrogen and stored at $-80 \text{ }^\circ\text{C}$ for further experiments.

Serum retinol detection

As described previously,⁸ the serum retinol levels were measured using high-performance liquid chromatography (HPLC) methods.

Transmission electron microscopy (TEM)

The proximal colon samples were harvested and fixed with glutaraldehyde and osmic acid. The changes in apical junctional complexes were observed using TEM. Image J software (NIH, Bethesda, MD, USA) was used to measure the length of desmosome junctions and the width of adherent junctions.

Serum diamine oxidase (DAO) measurement

The concentration of serum DAO was determined using an enzyme-linked immunosorbent assay under the manufacturer's protocol (Jiang Lai Biotech, China).

DNA extraction and PCR amplification

The cecum contents of the offspring rats were collected. Total microbial genomic DNA from the cecum contents was extracted as described previously.⁸ The hypervariable V3–V4 region of the 16s rDNA gene was amplified using a PCR thermocycler system (GeneAmp® 9700, ABI, CA, USA) with the primer pairs 338F (5'-ACTCCTACGGGAGGCAGCAG-3') and 806R (5'-GGACTACHVGGGTWTCTAAT-3').

Illumina MiSeq sequencing and processing of the sequencing data

Paired-end sequencing programs using the Illumina MiSeq PE300 platform/NovaSeq PE250 platform (Illumina, San Diego, CA, USA) were conducted on the above-purified PCR products following the manufacturer's standard protocols. Raw FASTQ files were de-multiplexed using an in-house Perl script, and then quality-filtered using FASTP software (<https://github.com/OpenGene/fastp>, version 0.19.6) and merged using FLASH software (<http://www.cbcb.umd.edu/software/flash>, version 1.2.11) with previously described criteria.⁸

Quantification of SCFAs

The colonic contents of the offspring rats were used to quantify the amounts of SCFAs. 50 ± 5 mg of colonic contents dissolved in 2 mL dH₂O was mixed by vortex. The mixtures were homogenized in a ball mill for 4 min, treated with ultrasound for 5 min, incubated in ice water, and then centrifuged at 5000 rpm for 20 min at 4 °C. Then, 0.8 mL of the supernatant was transferred into a fresh 2-mL microfuge tube, added with the internal standard, vortex-mixed for 10 s, oscillated for 10 min, treated with ultrasound for 5 min, centrifuged at 10,000 rpm under 4 °C for 15 min, and incubated at –20 °C for 30 min. Then, the supernatant was transferred into a fresh 2-mL glass vial for gas chromatography-mass spectrometry analysis.

RNA extraction

Total RNA was extracted from the colon tissue of the offspring rats. The quality and quantity of the RNA were measured using a 2100 Bioanalyser (Agilent Technologies,

USA) and ND-2000 (NanoDrop Technologies, USA), respectively.

Library preparation and sequencing

Total RNA (1 µg) was used to construct the transcriptome library according to the TruSeq™ RNA sample preparation Kit from Illumina (San Diego, CA). After quantification using a TBS380 mini fluorometer, the paired-end RNA-seq sequencing library was sequenced with the Illumina NovaSeq 6000 sequencer.

Differential expression analysis and functional enrichment

RNA sequencing (RNA-Seq) by expectation-maximization (RSEM, <http://deweylab.biostat.wisc.edu/rsem/>) was used to quantify gene abundance. Differentially expressed genes (DEGs) were selected using DESeq2. The significant DEGs were defined using the following criteria: $|\log_2(\text{fold-change})| \geq 0.58$ and $P \text{ value} \leq 0.05$ (DESeq2). In addition, functional-enrichment analysis including gene ontology (GO, <http://www.geneontology.org>, $P < 0.05$) and gene set enrichment analysis (GSEA, <http://software.broadinstitute.org/gsea/index.jsp>, $|\text{normalized enrichment score (NES)}| > 1$, nominal (NOM) $P \text{-value} < 0.05$, false discovery rate (FDR) $q \text{ value} < 0.25$) was performed to identify which functions and pathways correlated significantly with the DEGs compared with the whole-transcriptome background.

Quantitative real-time reverse transcription PCR

Total RNA was extracted from the colon tissue of male offspring rats or Caco-2 cells according to the protocol of the RNA extraction kit. The RNA was reversed transcribed to cDNA, which was used as the template for quantitative real-time PCR using the CFX96 real-time PCR detection system (Bio-Rad, USA). The primers sequence used were as follows: *Gapdh* (rat) forward, 5'-CCTGGAGAAACCTGCCAAG-3'; *Gapdh* (rat) reverse, 5'-CACAGGAGACAACCTGGTCC-3'; *Ceacam1* (rat) forward, 5'-GTGATTGGATCTGTGGCTGGAGTG-3'; *Ceacam1* (rat) reverse, 5'-GTGGCTGGAGGTTGAGGGTTTG-3'; *ACTB* (human) forward, 5'-GTGAAGGTGACAGCAGTCGGTT-3'; *ACTB* (human) reverse, 5'-GAGAAGTGGGGTGGCTTT-TAGGA-3'; *CEACAM1* (human) forward, 5'-CAACAGGACCA-CAGTCAAGACGATC-3'; *CEACAM1* (human) reverse, 5'-TGGAGCAGGTCAGGTTACAGAG-3'.

Western blotting

The nuclear protein samples from the colon were prepared according to the kit's instructions (Epigentek, USA). The total protein samples of the colon and cells were extracted using a radioimmunoprecipitation assay buffer containing phenylmethylsulfonyl fluoride. Protein samples were separated by sodium dodecyl sulfate-polyacrylamide gel electrophoresis and then transferred to polyvinylidene fluoride membranes (Millipore, USA). The membranes incubated with the primary antibodies, including those recognizing histone deacetylase 1 (HDAC1) (1:1000, ET1605-35, HuaBio, China), HDAC2 (1:1000, ET1607-78, HuaBio), HDAC3

(1:1000, ET1610-5, HuaBio), HDAC8 (1:1000, ET1612-90, HuaBio), CEA cell adhesion molecule 1 (CEACAM1) (1: 1000, A11626, Abclonal, China), proliferating cell nuclear antigen (PCNA) (1:1000, 200,947-6B12, Zenbio, USA) and Glyceraldehyde-3-phosphate dehydrogenase (GAPDH) (1:10,000, HRP60004, Proteintech, USA) at 4 °C overnight. After incubation with the appropriate secondary antibodies, the immunoreactive protein bands were detected using the ChemiDoc Imaging System (Bio-Rad).

Caco-2 cell culture

The human colon carcinoma cell line, Caco-2, was obtained from the Cell Bank, Chinese Academy of Sciences. The Caco-2 cells were cultured with Dulbecco's Modified Eagle's Medium (DMEM, Gibco, USA) containing 10% fetal bovine serum (FBS, Cellmax, China) in a CO₂ cell incubator at 37 °C.

Cell exposure to butyrate

The cells were exposed to butyrate at different concentrations for different durations. Cells in the control group were exposed to phosphate buffer. The cells were collected and used for RNA or protein extraction.

Chromatin immunoprecipitation (ChIP)

Caco-2 cells were treated with phosphate-buffered saline (PBS) or 2 mM butyrate for 24 h. ChIP assays were performed according to the instructions of the manufacturer (ABclonal). The cross-linked chromatin samples were separately incubated with antibodies recognizing HDAC1 (1:50, 34589s, CST, USA), HDAC3 (1:50, 85057s, CST), histone 3 (H3), and immunoglobulin G (IgG) (ABclonal) at 4 °C for 3 h, and then the complexes of antibodies and target proteins were incubated with protein A/G magnetic beads at 4 °C for 2 h. The immunoprecipitation complexes were washed and dissociated from the beads. The DNA was purified using an AFTSpin Multifunction DNA Purification Kit (ABclonal). Finally, qPCR was used to analyze the enriched DNA employing specific primers as follows: *CEACAM1-1* (human) forward: 5'-AGCCACCTCTGTCCACCTTCCTG-3'; *CEACAM1-1* (human) reverse: 5'-CAACACAGTGAGCTGCCAGGTC-3'; *CEACAM1-2* (human) forward: 5'-GGCTTTGCTAAGGAGGTGAAGGTAG-3'; *CEACAM1-2* (human) reverse: 5'-CCAGGAAGGGACAGAGCAGGTAC-3'; *CEACAM1-3* (human) forward: 5'-TTCTGTTCTAGCCCACTTCC-3'; *CEACAM1-3* (human) reverse: 5'-AAAACAAAGGCCAGTGAGG-3'.

Statistical analysis

Data were analyzed using GraphPad Prism software (version 8.3.0, GraphPad Inc., La Jolla, CA, USA). All data are represented as mean ± standard error of the mean (SEM). Comparisons among three groups were made using one-way analysis of variance (ANOVA) followed by Tukey's multiple comparisons tests. Comparisons between the two groups were made by unpaired *t*-test. The statistical significance level was set as $P < 0.05$.

Results

VAD during pregnancy inhibited the body weight growth and impaired the colonic epithelial barrier of offspring rats, which could be restored by postnatal VAS

To determine whether we successfully established the rat model of VAN, VAD, and VAS, the serum retinol concentration of those three groups was first measured by HPLC. As shown in [Figure 1A](#), the serum retinol concentration was lower in the rats of the VAD group than in the VAN group ($P = 0.006$). Moreover, the serum retinol concentration in the VAS group was significantly higher than that of the VAD group ($P = 0.003$). The results showed that the VAD diet successfully caused VAD in rats, and postnatal VAS could greatly prevent VAD in offspring. As VA strongly influences body growth and development, we next compared the body weight among the VAN, VAD, and VAS groups. [Figure 1B](#) shows that the VAD rats had much lower body weights than the VAN rats ($P < 0.001$), and the VAS rats were slightly heavier than the VAD rats ($P < 0.001$), but still had a lower body weight compared with those in the VAN group ($P < 0.001$). The above data demonstrated that serum retinol levels and body weight gain were inhibited by VAD. However, they were effectively improved by VAS in postnatal early life.

The mechanical barrier is the gut's first line of innate immune defense.¹⁶ To determine the effect of VAD on colonic cell-to-cell junctions, the apical junction complexes in the colon epithelium of the VAN, VAD, and VAS rats were observed using TEM. The desmosome junctions in the rats of the VAD group had shorter lengths and looser fibrils compared with those of the VAN and VAS groups ([Fig. 1C](#)). Then, we measured the length of the desmosome junctions and the width of adhesion junctions between adjacent colon epithelium cells to quantify the change in cell junctions. As shown in [Figure 1D](#), the desmosome junctions were shorter in the VAD group than in the both VAN and VAS groups ($P = 0.0176$ and $P = 0.0125$, respectively). Although no statistical differences were observed among these three groups, the width of adhesion junctions showed an increasing trend in the VAD group compared with those in the VAN and VAS groups ([Fig. 1E](#)). To verify the impairment of gut epithelial integrity, we measured the concentration of DAO. Rats in the VAD group had a higher concentration of serum DAO compared with that in the VAN and VAS groups ($P = 0.0306$ and $P = 0.0285$, respectively; [Fig. 1F](#)), which proved that VAD caused a leaky gut, and postnatal VAS decreased the gut epithelial permeability. The results indicated that VAD seriously damages gut epithelial barrier integrity, potentially by impairing the desmosome junctions, as indicated by their shortened length and loosened fibrils. Meanwhile, VAS in postnatal early life effectively protects desmosome junctions and gut epithelial integrity.

VAD during pregnancy modulated gut microbiota structure and alpha diversity

The gut microbiota, also called the microbial barrier, is another protective barrier for intestinal homeostasis.

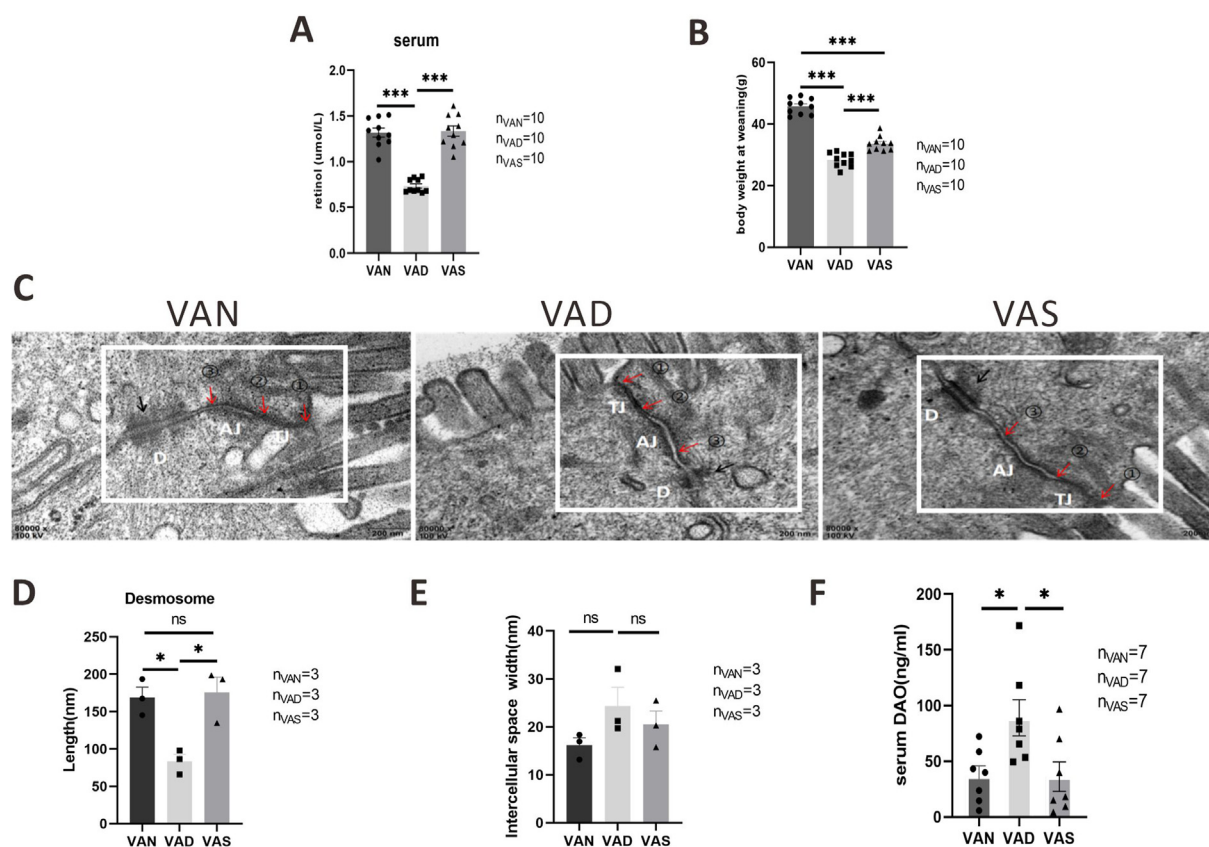


Figure 1 Effects of VAD and VAS on the weight and colonic epithelial barrier integrity. The alterations in (A) serum retinol concentration ($n = 10$ per group), (B) body weight ($n = 10$ per group), (C) ultrastructure of apical junction complex, (D) the length of desmosome junctions, (E) intercellular space width ($n = 3$ per group), and (F) serum DAO concentrations of offspring rats with different VA levels ($n = 7$ per group). Values are presented as the mean \pm SEM. Significance was tested using one-way ANOVA. * $P < 0.05$, *** $P < 0.001$; ns, not significant. VAN, vitamin A normal group; VAD, vitamin A deficiency group; VAS, vitamin A supplementation group; D, desmosome; TJ, tight junction; AJ, adhesion junction; DAO, diamine oxidase.

Studies have demonstrated the critical effects of the gut microbiota in modulating gut mechanical, chemical, and immune barriers, the mechanism of which might correlate with various metabolites, such as SCFAs,¹⁷ secondary bile acids,¹⁸ or tryptophan.¹⁹ To study the modulation by VAD on the gut microbiota composition, 16S rDNA sequencing was used to analyze the bacterial community structure and alpha diversity of cecum contents. Firstly, both principal coordinate analysis (PCoA) and non-metric multidimensional scaling (NMDS) analysis at the operational taxonomic unit (OTU) level revealed that the gut microbiome structures of the VAN, VAD, and VAS groups were notably different. PCoA showed that samples from the VAN, VAD, and VAS groups were markedly separated based on the first two principal components scores (PC1 and PC2), accounting for 26.92% (PC1) and 15.31% (PC2) of the explained variances (Fig. 2A). The NMDS analysis also displayed that the samples among different groups were dispersed based on NMDS1 and NMDS2 (Fig. 2B). Moreover, analysis of similarities (ANOSIM) revealed that the differences among the three groups were significantly greater than differences within the groups ($R^2 = 0.4957$, $P = 0.001$; Fig. 2A, B). In addition, partial least squares discriminant analysis (PLSDA) suggested that the serum retinol level was a fine group effector to discriminate the microbiome structure among

the three groups (Fig. 2C). Then, community richness and diversity were calculated using alpha diversity indexes. As shown in Figure 2D, the Ace, Chao, and Sobs indexes, as indicators of community richness, were significantly lower in the VAD group than in the VAN group ($P = 0.0024$, $P = 0.0030$, $P = 0.0064$, respectively), while no significant differences were found for above three indexes between the VAS and VAD groups. Simpson and Shannon's indexes are another two alpha diversity indexes, in which the former is negatively correlated, while the latter is positively correlated, with community diversity. In Figure 2E, the Simpson index in the VAD group was greater than that in the VAS group but was similar to that in the VAN group. However, the Shannon index was not significantly different among the groups (Fig. 2F). The above results indicated that VAD alters gut microbiome structure as well as its community richness and diversity.

VAD during pregnancy altered the gut microbiota composition and the relative abundance of SCFA-producing bacteria

To determine the detailed alterations in the gut microbiota composition and whether the relative abundance of SCFA-

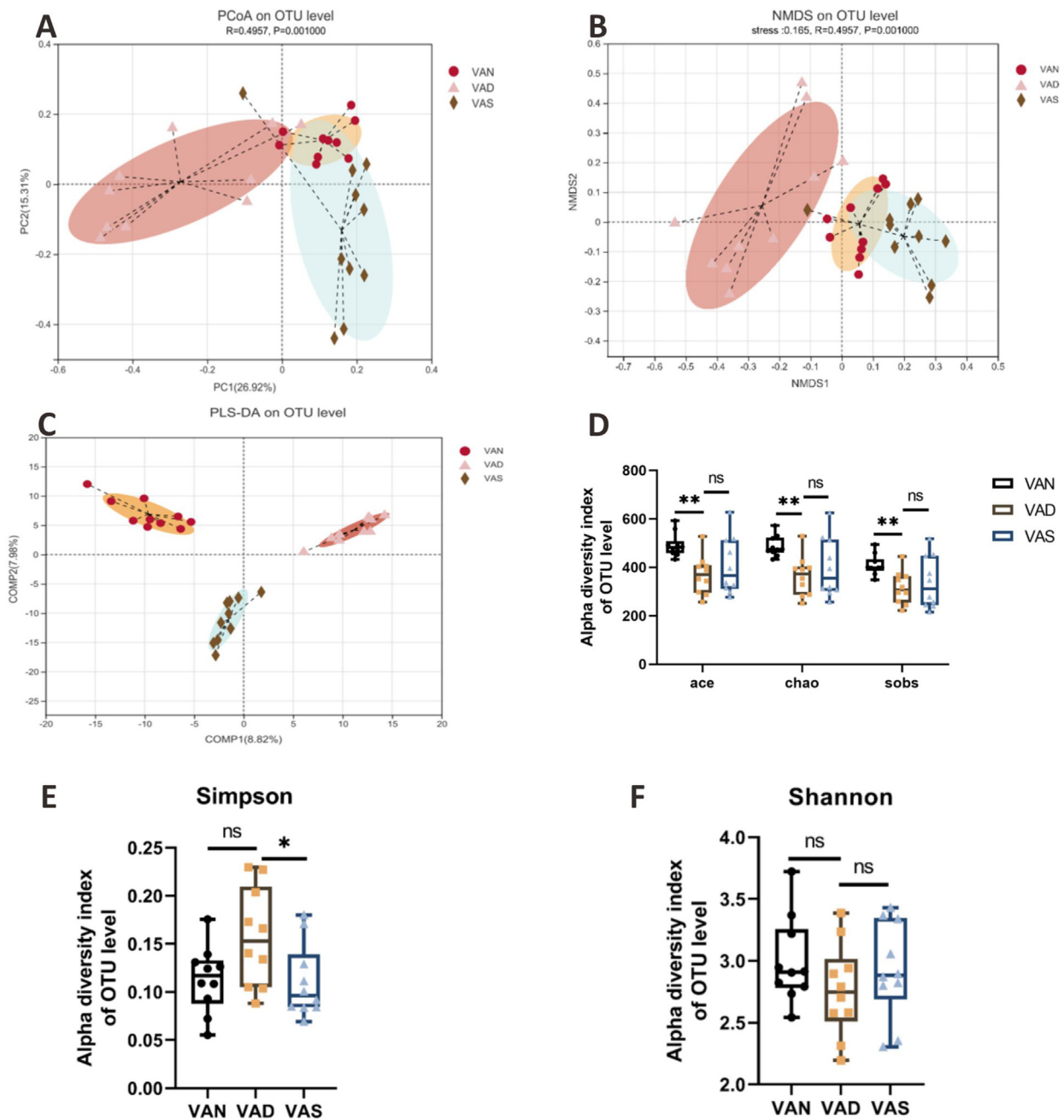


Figure 2 Effects of VAD and VAS on the structure of the gut microbiota. (A–C) Principal coordinate analysis (A), non-metric multidimensional scaling analysis (B), and partial least squares discriminant analysis (C) of the gut microbiota from the VAN, VAD, and VAS groups at the operational taxonomic unit level. (D–F) Comparison of Ace, Chao, and Sobs indexes (D), Simpson index (E), and Shannon index (F) of the gut microbiota from the VAN, VAD, and VAS groups. $n = 10$ per group; values are presented as the mean \pm SEM. Significance was tested with one-way ANOVA. * $P < 0.05$, ** $P < 0.01$; ns, not significant.

producing bacteria was modulated by VA, we analyzed the community composition at the phylum, family, and genus levels in the VAN, VAD, and VAS groups. The predominant phyla in the VAN group were Firmicutes (84.02%), Bacteroidota (5.72%), Actinobacteriota (4.49%), Verrucomicrobiota (3.46%), Desulfobacterota (1.17%), and Proteobacteria (0.36%). However, Firmicutes (60.25%), Verrucomicrobiota (14.47%), Bacteroidota (13.74%), Proteobacteria (9.26%), Actinobacteriota (1.14%), and

Desulfobacterota (0.88%) were the predominant phyla in the VAD group. Notably, Firmicutes (83.71%), Actinobacteriota (8.13%), Verrucomicrobiota (3.72%), Bacteroidota (2.31%), Proteobacteria (1.33%), and Desulfobacterota (0.17%) were the predominant phyla in the VAS group. The relative abundances of Firmicutes and Actinobacteriota in the VAD group were significantly decreased compared with those in the VAN group and were significantly increased in the VAS group compared with

those in the VAD group. In contrast, the relative abundance of Bacteroidota in the VAD group was greatly increased compared with that in the VAN and VAS groups (Fig. 3A). However, there were no differences in the ratio of Firmicutes to Bacteroidota among the VAN, VAD, and VAS three groups (Fig. 3B).

At the family level, we noticed that the Lactobacillaceae family was the most abundant among the VAN

(44.55%), VAD (33.76%), and VAS (35.96%) groups. The top 10 microflora at the family level, the relative abundance of which changed significantly, as determined by one-way ANOVA analysis, among the VAN, VAD, and VAS groups are shown in Figure 3C. Surprisingly, we found that Peptostreptococcaceae (6.54% vs. 14.05%), Erysipelotrichaceae (0.84% vs. 6.74%), Coriobacteriaceae (0.20% vs. 4.21%), Eggerthellaceae (0.08% vs. 0.16%), and Staphylococcaceae

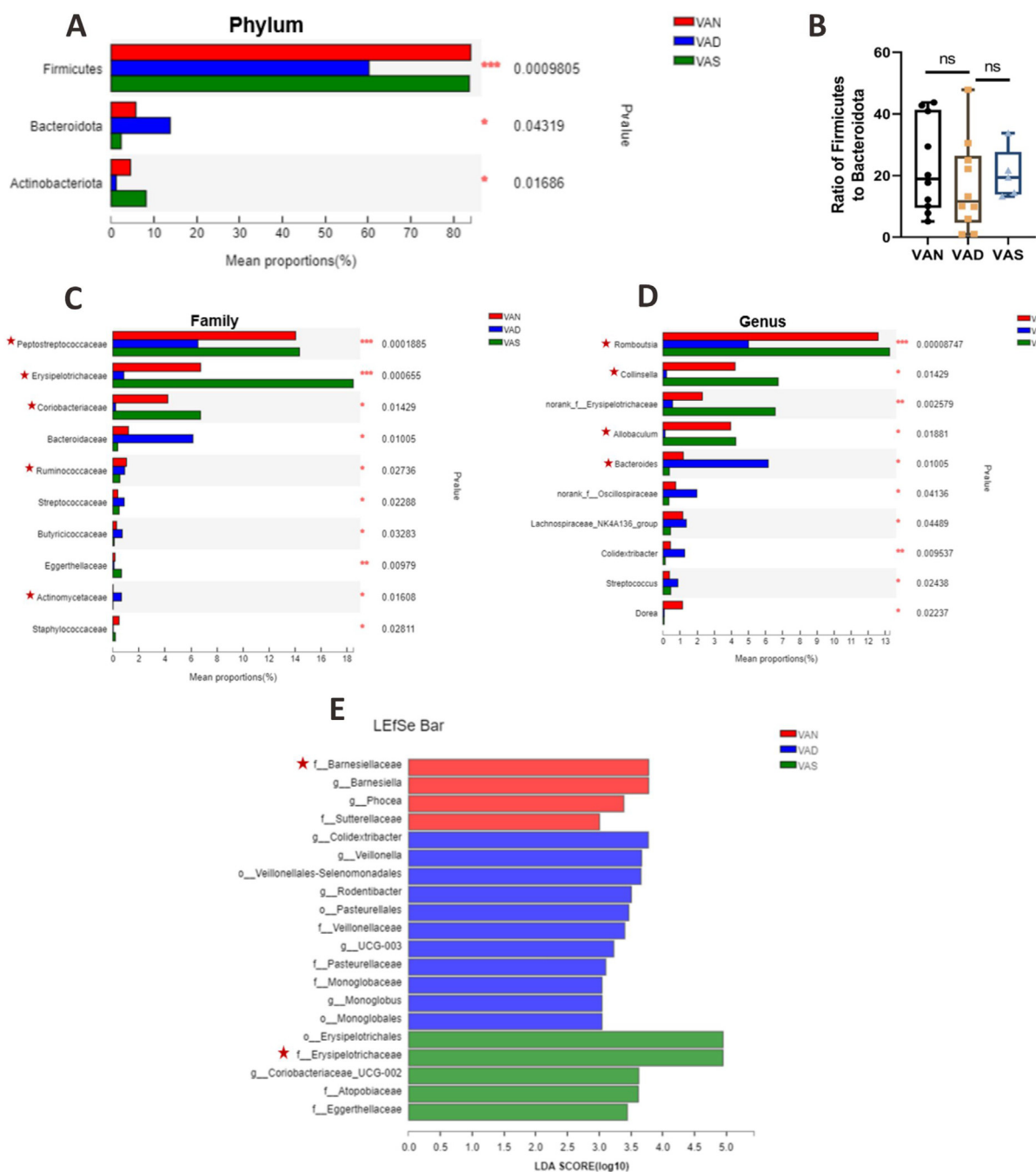


Figure 3 Effects of VAD and VAS on the composition of the gut microbiota and the relative abundance of SCFA-producing bacteria. (A–D) The difference in (A) phylum level, (B) the ratio of F/B, (C) family level, and (D) genus level based on the one-way ANOVA. (E) Least discriminant analysis (LDA) score distribution for the most abundant phylotypes from the cecum microbiota of the VAN, VAD, and VAS groups. SCFA-producing bacteria are marked with red stars. $n = 10$ per group; values are presented as the mean \pm SEM. Significance was tested with one-way ANOVA. $*P < 0.05$, $**P < 0.01$, $***P < 0.001$; ns, not significant.

(0.02% vs. 0.46%) were significantly decreased in the VAD group compared with those in the VAN group, while they were greatly increased in the VAS group (14.35% vs. 6.54%, 18.48% vs. 0.84%, 6.73% vs. 0.20%, 0.65% vs. 0.08%, 0.18% vs. 0.02%). In contrast, Bacteroidaceae (6.15% vs. 1.18%, 0.36%), Streptococcaceae (0.86% vs. 0.37%, 0.47%), Butyricoccaceae (0.71% vs. 0.28%, 0.09%), and Actinomycetaceae (0.65% vs. 0.01%, 0.01%) in the VAD group were significantly increased compared with those in both the VAN and VAS groups.

Lactobacillus, belonging to the Lactobacillaceae family, was the most abundant microflora genus in the VAN (44.55%), VAD (33.76%), and VAS (35.96%) groups. The top 10 microflora at the genus level, the relative abundance of which changed significantly among the VAN, VAD, and VAS groups, are displayed in Figure 3D. The relative abundances of *Romboutsia* (4.99% vs. 12.58%), *Collinsella* (0.20% vs. 4.22%), *norank_f_Erysipelotrichaceae* (0.55% vs. 2.30%), and *Allobaculum* (0.11% vs. 3.95%) in the VAD group were significantly lower than those in the VAN group, while their abundances in the VAS group were significantly higher than those in the VAD group (13.25% vs. 4.99%, 6.73% vs. 0.20%, 6.56% vs. 0.55%, 4.25% vs. 0.11%). However, the relative abundance of *Bacteroides* (6.15% vs. 1.18%, 0.36%), *norank_f_Oscillospiraceae* (1.97% vs. 0.73%, 0.33%), *Lachnospiraceae_NK4A136_group* (1.36% vs. 1.15%, 0.43%), *Colidextribacter* (1.26% vs. 0.42%, 0.12%), and *Streptococcus* (0.86% vs. 0.37%, 0.44%) in the VAD group were significantly higher than those in the VAN and VAS groups.

Linear discriminant analysis Effect Size (LEfSe) was used to further identify the key phylotypes responsible for the differences among the VAN, VAD, and VAS groups. As shown in Figure 3E, *f_Barnesiellaceae*, *g_Barnesiella*, *g_Phocaea*, and *f_Suttereuaceae* were identified as key phylotypes to discriminate the VAN group from the VAD and VAS groups. Three phylotypes at the order level (*o_Veillonellales-Selenomonadales*, *o_Pasteurellales*, *o_Monoglobales*), three phylotypes at the family level (*f_Veillonellaceae*, *f_Pasteurellaceae*, *f_Monoglobaceae*), and five phylotypes at the genus level (*g_Colidextribacter*, *g_Veillonella*, *g_Rodentibacter*, *g_UCG-003*, *g_Monoglobus*) were identified as key phylotypes to discriminate the VAD group from the VAN and VAS groups. In the VAS group, the key phylotypes were *o_Erysipelotrichales*, *f_Erysipelotrichaceae*, *g_Coriobacteriaceae_UCG-002*, *f_Atopobiaceae*, and *f_Eggerthellaceae*.

The above results demonstrated that the microbiota composition was influenced by VAD, while VAS in postnatal early life could prevent disorders in the relative abundance of key microbiota. The microflora modulated by VAD and the key phylotypes in the VAN, VAD, and VAS group were identified; therefore, the SCFA-producing bacteria were identified and marked with red stars (Fig. 3C–E). At the family level, SCFA-producing bacteria, including Peptostreptococcaceae,²⁰ Erysipelotrichaceae,²¹ Coriobacteriaceae,²² and Ruminococcaceae²¹ were decreased in the VAD group, while the above bacteria in the VAS group, except Ruminococcaceae, were increased. However, valeric acid-associated bacteria Actinomycetaceae²¹ increased in the VAD group and decreased in both the VAS and VAN groups (Fig. 3C). At the genus level, *Romboutsia*²³, *Collinsella*²⁴, and *Allobaculum*²⁵ among the SCFA-producing bacteria decreased and

*Bacteroides*²⁶ increased in the VAD group (Fig. 3D). Furthermore, *f_Barnesiellaceae*, the key bacteria in the VAN group, was reported to be positively correlated with butyrate and total SCFAs.²⁷ In addition, *f_Erysipelotrichaceae*,²¹ the key bacteria in the VAS group, is an SCFA-producing bacteria (Fig. 3E). Taken together, the reported and our current study indicated that the gut microbiota composition, especially the relative abundance of SCFA-producing bacteria taxa, is greatly influenced by VAD and is ameliorated by postnatal VAS.

VAD during pregnancy reduced the SCFA content and proportion in colonic contents, which were restored by postnatal VAS

Gut microorganisms ferment dietary fiber and protein to produce SCFAs, mainly including acetic acid, propionic acid, butyric acid, isobutyric acid, valeric acid, and iso-valeric acid. As shown in Figure 4A, the number of total SCFAs was significantly reduced in the VAD group compared with that in the VAN group ($P = 0.0004$) but was markedly increased in the VAS group ($P = 0.0009$). Moreover, compared with both the VAN and VAS groups, the VAD group presented a lower concentration of acetic acid ($P = 0.0333$ and $P = 0.0197$, respectively), propionic acid ($P = 0.0014$ and $P = 0.0025$, respectively), butyric acid ($P < 0.0001$ and $P = 0.0003$, respectively), isobutyric acid ($P = 0.0001$ and $P < 0.0001$, respectively), valeric acid ($P < 0.0001$ and $P = 0.0008$, respectively), and iso-valeric acid ($P < 0.0001$ and $P = 0.0028$, respectively) (Fig. 4B–G).

To further analyze the impact of VA on the composition of total SCFAs, the proportion of acetic acid, propionic acid, butyric acid, isobutyric acid, valeric acid, and iso-valeric acid among total SCFAs was calculated (Fig. 4H). The proportions of propionic acid ($P = 0.0014$ and $P = 0.0054$, respectively), butyric acid ($P = 0.0005$ and $P = 0.0472$, respectively), and isobutyric acid ($P = 0.0257$ and $P = 0.0009$, respectively) in the VAD group were lower than those in the VAN and VAS groups (Fig. 4J–L), while the proportion of acetic acid ($P < 0.001$ and $P < 0.001$, respectively) was significantly higher in the VAD group (Fig. 4I). However, the proportions of valeric acid and iso-valeric acid were not significantly different among the three groups (Fig. 4M, N).

Accordingly, we proposed that VAD could reduce SCFA metabolites, as well as decrease the ratio of propionic acid, butyric acid, and isobutyric acid among the total SCFAs. In the meantime, postnatal VAS reversed the changes in the absolute and relative amounts of colonic SCFAs.

VAD during pregnancy affected different genes related to colonic barrier function

Transcriptome sequencing of the colon was conducted to find target functionally enriched pathways and different genes affected by VAD. Figure 5A shows the principal component analysis (PCA) of the colonic transcriptome expression model in rats among the VAN, VAD, and VAS groups. Then, we analyzed the number of DEGs between the VAN and VAD groups and between the VAD and VAS

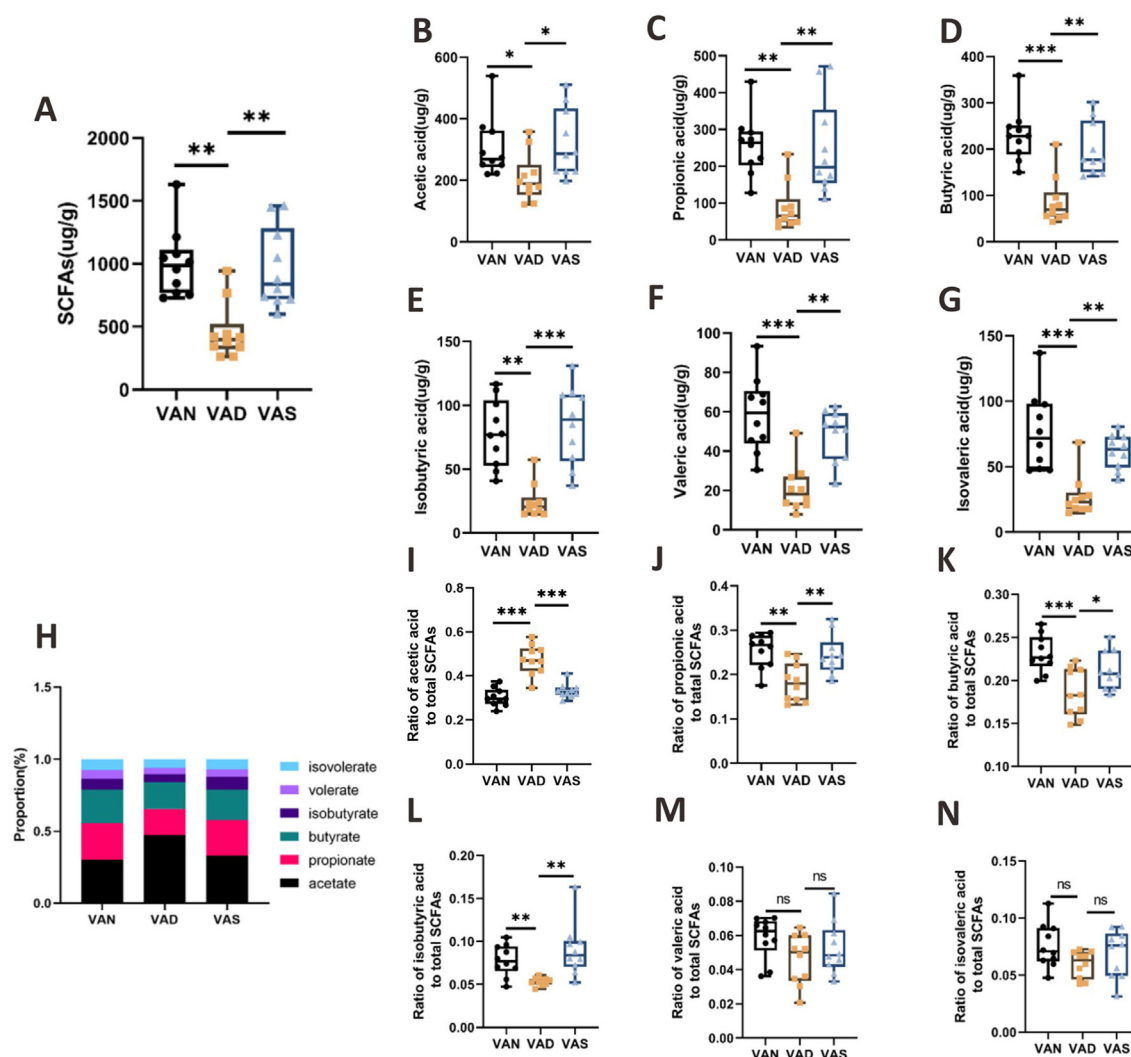


Figure 4 Effects of VAD and VAS on short-chain fatty acids. (A) Total short-chain fatty acids; (B) acetic acid; (C) propionic acid; (D) butyric acid; (E) isobutyric acid; (F) valeric acid; (G) isovaleric acid. (H) The proportion of separate short-chain fatty acids in total short-chain fatty acids. (I–N) The ratios of (I) acetic acid, (J) propionic acid, (K) butyric acid, (L) isobutyric acid, (M) valeric acid, and (N) isovaleric acid to total SCFAs. $n = 10$ per group; values are presented as the mean \pm SEM. Significance was tested with one-way ANOVA. * $P < 0.05$, ** $P < 0.01$, *** $P < 0.001$; ns, not significant.

groups. As shown in Figure 5B, there were 825 DEGs between the VAN and VAD groups and 2157 DEGs between the VAD and VAS groups. In detail, compared with the VAN group, the VAD group had 355 significantly up-regulated genes, and 470 significantly down-regulated genes. However, compared to the VAD group, the VAS group had 913 significantly up-regulated genes and 1244 down-regulated genes.

To further analyze the functions of identified DEGs among the VAN, VAD, and VAS groups, GO analysis was conducted. We found that both the DEGs between the VAN and VAD groups and between the VAD and VAS groups were all enriched in GO categories related to the gut barrier function in the biological process (Fig. 5C, D), molecular function (Fig. 5E, F), and cellular component (Fig. 5G, H) categories. Interestingly, DEGs between the VAN and VAD group were enriched in cell adhesion molecule binding, apical plasma membrane, anchoring junction, and cell–cell

junction, and DEGs between the VAD and VAS group also enriched in adherens junction organization, cell–cell junction organization, cell adhesion molecule binding, apical plasma membrane, anchoring junction, and junctional membrane complex. These data indicated that the colonic transcriptome and gene expression levels associated with gut barrier function are impacted by different VA levels.

VAD during pregnancy decreased CEACAM1 and increased HDAC1 and HDAC3 expression levels

A Venn diagram suggested that the DEGs between the VAN and VAD groups and those between the VAD and VAS groups shared 25 common genes related to the gut barrier (Fig. 6A). Among them, the *Ceacam1* expression level decreased in the VAD group compared with that in the VAN group, while it increased in the VAS group (Fig. 6B).

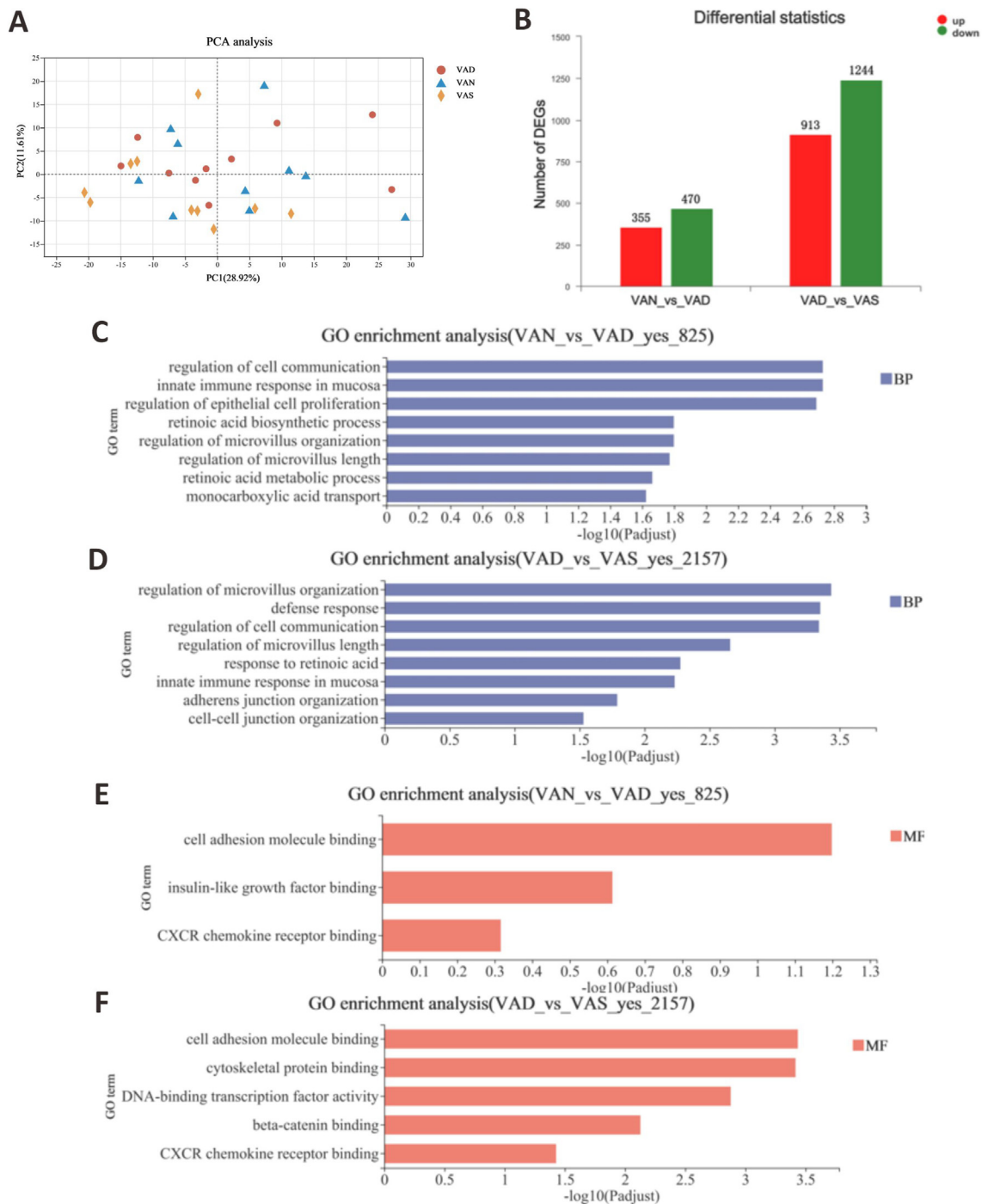


Figure 5 Effects of VAD and VAS on the colonic transcriptome. (A) Principal component analysis of the colonic transcriptome expression of rats from the VAN, VAD, and VAS groups. (B) Numbers of differentially expressed genes (DEGs) between the VAN and VAD groups, and between the VAD and VAS groups. (C–H) (C, D) GO_BP enrichment analysis, (E, F) GO_MF enrichment analysis, and (G, H) GO_CC enrichment analysis for DEGs between the VAN and VAD groups, and between the VAD and VAS groups. $n = 10$ per group; DEGs were identified according to $|\log_2(\text{fold-change})| \geq 0.58$ and a P value ≤ 0.05 (DESeq2). BP, biological process; MF, molecular function; CC, cellular component.

Moreover, the result of qRT-PCR was consistent with that of the transcriptome sequencing (Fig. 6D). Western blotting revealed that the protein level of CEACAM1 was significantly lower in the VAD group than in the VAN and VAS groups ($P = 0.0125$ and $P = 0.0111$, respectively;

Figure 6E, F). In general, VAD down-regulated the transcription and protein level of CEACAM1, and postnatal VAS promoted it. However, the mechanism was unclear.

SCFAs play a protective role in the gut barrier by inhibiting histone deacetylase to modulate gene expression

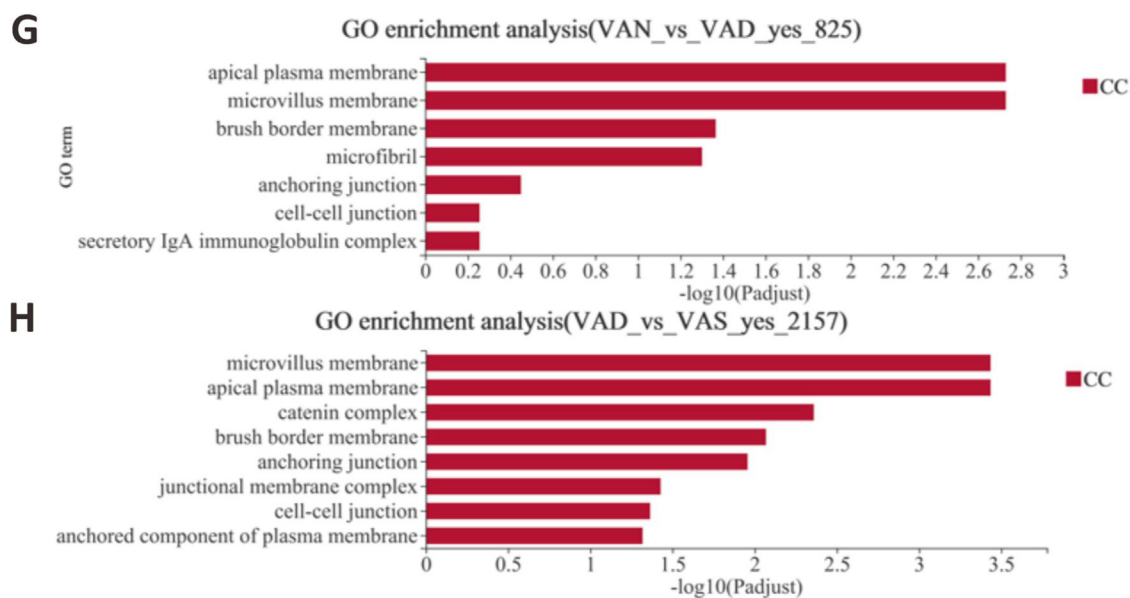


Figure 5 (continued).

levels. GSEA indicated that histone deacetylase complexes were enriched in the VAD group compared with those in the VAN group ($NES = 1.502$, P value = 0.006, P adjust value = 0.072; Fig. 6C). Therefore, we next detected the protein levels of HDACs, including HDAC1, HDAC2, HDAC3, and HDAC8 (Fig. 6G–K). The western blotting results showed that the relative levels of HDAC1 and HDAC3 were higher in the VAD group rats than in the VAN group, whereas their levels were significantly lower in the VAS group. Among the VAN, VAD, and VAS groups, there were no differences in the levels of HDAC2 and HDAC8. These results suggest that the decreased concentration of SCFAs caused by VAD might lead to increased deacetylation, which was reduced by postnatal VAS during the early-life period.

Butyrate inhibited the recruitment of HDAC3, not HDAC1, onto the *CEACAM1* promoter in Caco-2 cells

To determine whether SCFAs regulated *CEACAM1* expression via HDACs, we treated Caco-2 cells *in vitro* using sodium butyrate at different concentrations for different durations. qRT-PCR showed that butyrate promoted *CEACAM1* mRNA expression, which was dependent on the concentration of butyrate and the duration of treatment (Fig. 7A). There was no difference in the mRNA expression level of *CEACAM1* between the control and butyrate groups when Caco-2 cells were treated for 12 h. However, butyrate at 2, 3, and 4 mM for 24 or 30 h significantly increased the mRNA level of *CEACAM1* in Caco-2 cells. We found that there was an appropriate concentration of butyrate between 2 and 4 mM that promoted the mRNA expression of *CEACAM1*, while butyrate at 1 mM had no effect. Moreover, western blotting showed that butyrate treatment at 2 and 3 mM for 24 h significantly increased the protein levels of *CEACAM1* ($P = 0.0052$ and $P = 0.0284$, respectively; Fig. 7B, C). Meanwhile, the levels of HDAC1 and HDAC3 were reduced following butyrate treatment at 2 mM for 24 h ($P = 0.0183$ and $P = 0.0163$, respectively; Fig. 7D–F).

Furthermore, to determine whether HDAC1 or HDAC3 interacted with the *CEACAM1* gene promoter and was responsible for its expression, primers for different *CEACAM1* gene promoter regions (–302 bp to –389 bp, –809 bp to –905 bp, and –1294 bp to –1384 bp relative to the transcription start site (TSS)) were used for ChIP-qPCR in Caco-2 cells with or without butyrate exposure (Fig. 7G). The ChIP data revealed that the recruitment of HDAC3, but not HDAC1, onto the promoter regions of *CEACAM1* was significantly inhibited by butyrate in Caco-2 cells (Fig. 7H–M). These results provided evidence that butyrate promotes *CEACAM1* gene expression by inhibiting the recruitment of HDAC3, not HDAC1, onto its promoter.

Discussion

The mechanisms underlying the potential influence of SCFAs on gut epithelial barrier integrity during VAD have not been clarified. The present study first revealed that gestational VAD resulted in gut microbiota dysbiosis (especially of flora-producing SCFAs) in their offspring, which decreased SCFA levels. Decreasing SCFA levels (especially butyric acid) inhibited *CEACAM1* expression levels through HDAC to impair desmosome junctions in the apical epithelium. Nevertheless, VAS in the postnatal early-life period could reverse the decrease in *CEACAM1* expression by increasing SCFAs. The mechanistic study revealed that butyrate promoted *CEACAM1* expression by inhibiting the recruitment of HDAC3 to the *CEACAM1* promoter.

The significant functions of the gut microbiome in modulating gut homeostasis and the gut barrier have been studied extensively. In recent years, scholars have discovered that micronutrients (e.g., VA, vitamin C, vitamin E, vitamin D, folate, iron, and zinc) are closely relevant to the gut microbiota composition and the enrichment of particular bacterial taxa.²⁸ Interestingly, in one study on the effects of micronutrients (VA, folate, iron, and zinc) on the

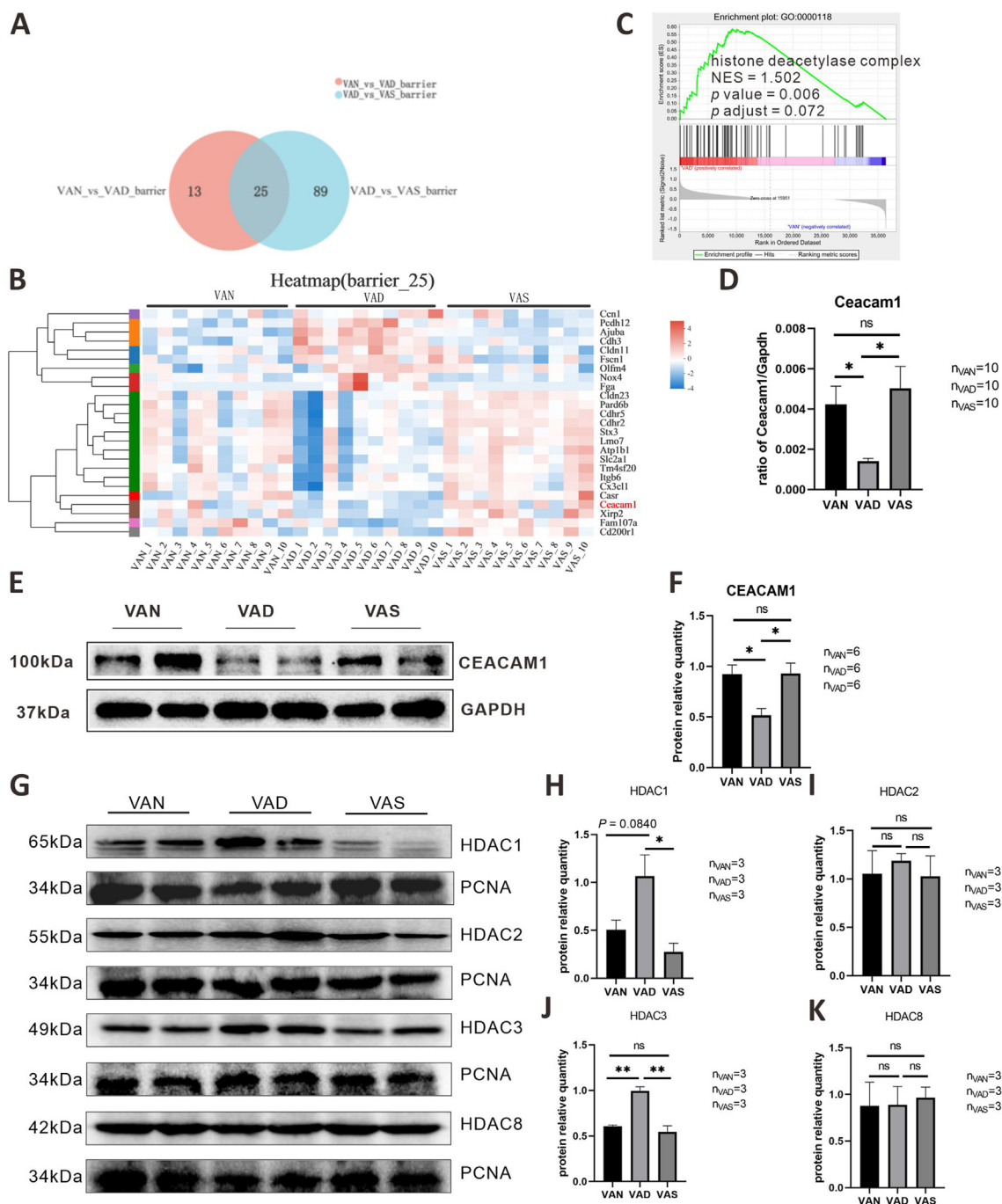


Figure 6 Effects of VAD and VAS on the expression of CEACAM1 and HDACs in the offspring's colon tissue. (A) Numbers of DEGs between the VAN vs. VAD groups and those between the VAD vs. VAS groups ($n = 10$ per group). (B) The heatmap of common DEGs ($n = 10$ per group). (C) GSEA analysis on histone deacetylase complex between the VAN and VAD groups ($n = 10$ per group). (D) Comparison of *Ceacam1* mRNA expression levels among the groups ($n = 10$ per group). (E) Western blotting analysis of CEACAM1 protein levels among the groups. (F) Comparison of CEACAM1 protein levels among the groups ($n = 6$ per group). (G) Western blotting analysis of HDAC1, HDAC2, HDAC3, and HDAC8 levels among the groups. (H–K) Comparison of HDAC1, HDAC2, HDAC3, and HDAC8 protein levels among the groups ($n = 3$ per group). Values are presented as the mean \pm SEM. Significance was tested with one-way ANOVA. * $P < 0.05$, ** $P < 0.01$; ns, not significant.

gut microbiome, researchers found that VA had the largest influence on bacterial community structure.²⁹ Firmicutes and Bacteroidetes are the two most abundant phyla of the gut microbiome in humans and animals. Changes in the

ratio of Firmicutes to Bacteroidetes have been identified in imbalanced gut microecology.^{30,31} Li and colleagues observed that the intake amount of beta-carotene, a precursor of vitamin A, correlated positively with Firmicutes

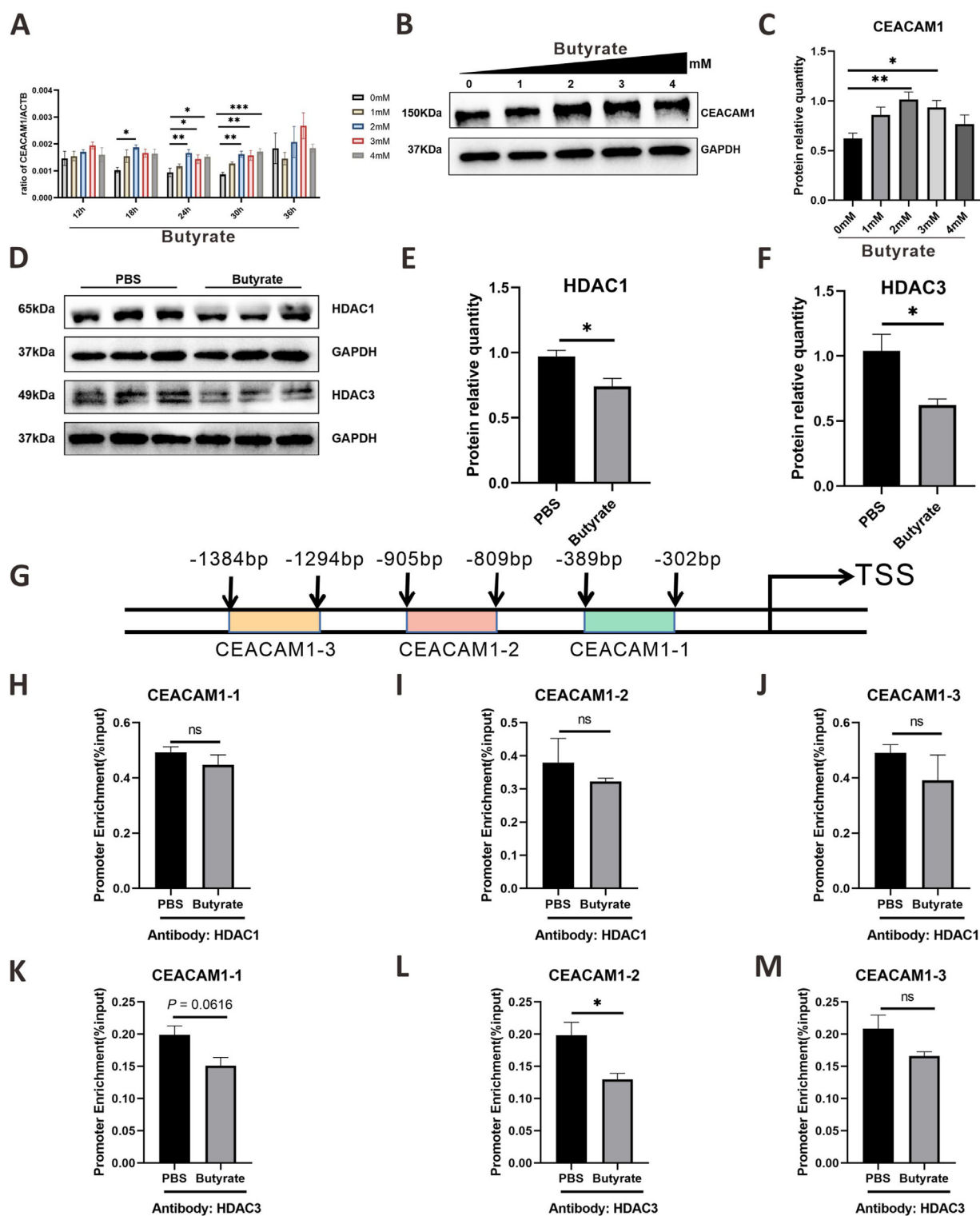


Figure 7 Butyrate inhibited the recruitment of HDAC3 to the promoter of *CEACAM1* in Caco-2 cells. **(A)** The changes in *CEACAM1* mRNA expression in cells exposed to butyrate at different concentrations and durations ($n = 5$ per group). **(B)** Western blotting analysis of *CEACAM1* protein levels in cells exposed to butyrate at different concentrations for 24 h. **(C)** Comparison of *CEACAM1* levels among groups ($n = 3$ per group). **(D)** Western blotting analysis of HDAC1 and HDAC3 protein levels in cells exposed to 2 mM butyrate for 24 h. **(E, F)** Comparison of HDAC1 and HDAC3 between the PBS group and the butyrate group ($n = 5$ per group). **(G)** Positions of ChIP-qPCR product fragments of primers for different promoter regions relative to the TSS. **(H–M)** ChIP-qPCR analysis of the enrichment of **(H–J)** HDAC1 and **(K–M)** HDAC3 on the different promoter regions of the *CEACAM1* gene in cells from the PBS and Butyrate groups ($n = 3$ per group). Values are presented as the mean \pm SEM. Significance was tested with an unpaired t -test. $*P < 0.05$; ns, not significant.

and negatively with Bacteroidetes in patients with cystic fibrosis.³² In the current study, we also found that persistent VAD at the beginning of pregnancy decreased the relative abundance of Firmicutes and increased the relative abundance of Bacteroidetes in the offspring. In addition, VAS in the postnatal early-life period effectively recovered the relative abundance of Firmicutes and Bacteroidetes and increased the ratio of Firmicutes to Bacteroidetes. Lee's study suggested that retinol and retinoic acid prevented norovirus replication by affecting the gut microbiome composition, especially by increasing the relative abundance of *Lactobacillus*.³³ Another work also observed that the relative abundance of *Lactobacillus* was decreased in the colon by VAD.³⁴ Our study found that Lactobacillaceae and *Lactobacillus* were the most abundant bacteria taxa at the family and genus levels in the VAN, VAD, and VAS groups. Moreover, the relative abundance of Lactobacillaceae and *Lactobacillus* was decreased in the VAD group but was increased by postnatal VAS.

The effects of VAD on gut microbiome composition have been reported previously. However, the influence of VAD and VAS on colonic SCFAs and SCFA-producing bacteria is less well known. Scholars have found that a major bioactive constituent of green tea ameliorated colonic barrier integrity and inhibited inflammation by enriching SCFA-producing bacteria, such as *Akkermansia*, and increasing SCFA production in dextran sulfate sodium (DSS)-induced colitis.³⁵ Moreover, intestinal injury caused by a high iron diet or radiation was correlated with the decrease in total SCFAs and SCFA-producing bacteria.³⁶ In our study, disturbances of SCFA levels and SCFA-producing bacteria abundance were observed in the colons of rats with different VA levels. Four bacteria (*Peptostreptococcaceae*, *Erysipelotrichaceae*, *Coriobacteriaceae*, and *Ruminococcaceae*) at the family level, and three (*Romboutsia*, *Collinsella*, and *Allobaculum*) at the genus level belonging to SCFA-producing bacteria taxa were decreased by VAD but increased following VAS. In contrast, one (*Actinomycetaceae*) at the family level and one (*Bacteroides*) at the genus level were enriched by VAD, but reduced by VAS. Similarly, gestational VAD decreased the absolute content of acetic acid, propionic acid, butyric acid, isobutyric acid, valeric acid, and isovaleric acid in the offspring colon, while VAS in the postnatal early-life period effectively prevented these reductions. Moreover, among the total SCFAs, except for the proportion of acetic acid, the proportions of propionic acid, butyric acid, and isobutyric acid were decreased by gestational VAD and increased by postnatal VAS. Accordingly, we first clarified that the decrease in SCFA levels during VAD might be caused by the alterations in gut bacteria composition, especially the depletion of the above SCFA producers.

SCFAs, especially butyric acid, have been reported to regulate gene expression by inhibiting histone deacetylases.^{37,38} To further investigate the potential mechanism by which the insufficient production of SCFAs led to disrupted colonic epithelial barrier function, we compared the levels of class I histone deacetylases, including HDAC1, HDAC2, HDAC3, and HDAC8, in colon tissue among offspring rats from the VAN, VAD, and VAS groups. The results revealed that the levels of HDAC1 and HDAC3 in the VAD group were significantly higher than those

in the VAN group, which might result from the decreased production of SCFAs. Surprisingly, following the elevation of colonic SCFAs by timely postnatal VAS, HDAC1, and HDAC3 levels were down-regulated to levels similar to those in the VAN group. A study showed that the reduction of butyrate-producing bacteria and inadequate butyrate alleviated HDAC3 inhibition to increase colon permeability.³⁹ In rat models of allergic rhinitis, a high HDAC1 protein level was proven to inhibit the tight junction protein, zonula occludens-1 (ZO-1).³⁹ Other studies showed that trichostatin A (TSA), an inhibitor of HDACs, increased tight junction protein levels, including cingulin (CGN) and ZO-3, by down-regulating the expression of p63.⁴⁰ Furthermore, HDAC3 inhibition increased the levels of VE-cadherin and claudin-5 to protect the integrity of the blood–brain barrier.⁴¹

By transcriptome sequencing, we found that pregnancy VAD and postnatal VAS affected colonic genes enriched in the gut epithelial barrier function, especially cell–cell junctions, in which *Ceacam1* was the most affected. CEACAM1 is highly expressed in colon epithelial cells⁴² and significantly modulates the intestinal immune response to infections and the integrity of the epithelial barrier.⁴³ Knockout of *Ceacam1* was reported to cause a dysregulated CD8⁺ T cell response and increase colonic epithelial permeability during *Citrobacter rodentium*-induced colitis.⁴³ Lack of CEACAM1 reduced intestinal IgA secretion and inhibited the host defense against pathogens such as *Listeria monocytogenes*.⁴⁴ In ulcerative colitis (UC) mice, the CEACAM1 expression was determined to be declined. Moreover, overexpression of *Ceacam1* was proven to play a protective role in the colonic epithelial barrier by promoting tight junction protein expression, decreasing the secretion of inflammatory factors, and down-regulating expression levels of cytochrome C oxidase II (COX2) and inducible nitrous oxide synthase (iNOS).⁴⁵ However, no studies have suggested the effects of VAD and VAS on colonic CEACAM1 expression and the underlying modulatory mechanism. The results of the present study revealed that both the mRNA and protein expression levels of CEACAM1 were decreased in the VAD group, while they were restored by VAS in the postnatal early-life period. According to a previous report, the transcription factor Sp2 recruits HDAC to repress transcription of the *CEACAM1* gene; however, the specific HDAC was not identified.⁴⁶ To further shed light on the regulatory mechanism among SCFAs, HDAC1, HDAC3, and CEACAM1, we treated Caco-2 cells *in vitro* using butyrate. Butyrate effectively up-regulated *CEACAM1* mRNA transcription activity and inhibited the protein expression levels of both HDAC1 and HDAC3 in Caco-2 cells. However, the ChIP-qPCR results confirmed that the recruitment of HDAC3, but not HDAC1, onto the *CEACAM1* gene promoter was suppressed by butyrate. The likely explanation is that the target genes of HDAC1 and HDAC3 are different, although they are known to down-regulate the transcriptional activity of target genes through the action of histone acetylation inhibition.⁴⁷ Meanwhile, this finding also motivates us to further clarify the detailed target genes that are regulated by HDAC1 in vitamin A deficiency.

Thus, VAD from the beginning of pregnancy triggered deacetylation of the colonic *CEACAM1* gene, thereby reducing its expression. This is mediated through decreasing SCFA concentrations and impairing desmosome

junctions of the apical epithelium in the offspring's colon. VAS in postnatal offspring successfully down-regulated HDAC3 expression levels via enriching SCFA-producing bacteria taxa, which increased CEACAM1 expression to enhance desmosome junctions between epithelium cells. However, the mechanism by which CEACAM1 modulates the colonic epithelial barrier requires further investigation.

Conclusion

Our research firmly supported that VAD from the beginning of pregnancy suppresses the production of colonic SCFAs in the offspring by decreasing the relative abundance of SCFA-producing gut microorganisms. This down-regulates colonic CEACAM1 expression by triggering HDAC3 levels, ultimately resulting in impaired apical epithelial integrity of the colon. Furthermore, timely VAS in the postnatal early-life period effectively up-regulated CEACAM1 expression to protect colonic epithelial integrity by reversing the disordered gut microbiota and the decrease in SCFAs.

Ethics declaration

The animal study was reviewed and approved by the Ethics Committee of the Children's Hospital of Chongqing Medical University.

Author contributions

JC designed the study and provided financial support for the study. JY conducted the experiments and analyzed the data. LX helped collect samples. DF and BC provided technical guidance during the experiments. TY guided the use of HPLC. BT and RL assisted in making the VAN and VAD diet. JC and JY wrote the manuscript. All authors contributed to the study and approved the final manuscript.

Conflict of interests

The research was conducted in the absence of any commercial or financial relationships that could be construed as a potential conflict of interests.

Funding

This work was supported by grants from The National Natural Science Foundation of China (No. 31971089), the General Project of Chongqing Natural Science Foundation (China) (No. CSTB2022NSCQ-MSX0107), and the Scientific Research Innovation Project for Postgraduates in Chongqing City (China) (No. CYS19198).

References

1. Zhao T, Liu S, Zhang R, et al. Global burden of vitamin A deficiency in 204 countries and territories from 1990-2019. *Nutrients*. 2022;14(5):950.
2. Biyong EF, Alfors S, Dumetz F, et al. Dietary vitamin A supplementation prevents early obesogenic diet-induced microbiota, and neuronal and cognitive alterations. *Int J Obes*. 2021;45(3):588–598.
3. Honarbakhsh M, Ericsson A, Zhong G, et al. Impact of vitamin A transport and storage on intestinal retinoid homeostasis and functions. *J Lipid Res*. 2021;62:100046.
4. Xiao L, Cui T, Liu S, et al. Vitamin A supplementation improves the intestinal mucosal barrier and facilitates the expression of tight junction proteins in rats with diarrhea. *Nutrition*. 2019;57:97–108.
5. Li Y, Gao Y, Cui T, et al. Retinoic acid facilitates toll-like receptor 4 expression to improve intestinal barrier function through retinoic acid receptor beta. *Cell Physiol Biochem*. 2017;42(4):1390–1406.
6. Liu X, Li Y, Wang Y, et al. Gestational vitamin A deficiency reduces the intestinal immune response by decreasing the number of immune cells in rat offspring. *Nutrition*. 2014;30(3):350–357.
7. Liu X, Cui T, Li Y, et al. Vitamin A supplementation in early life enhances the intestinal immune response of rats with gestational vitamin A deficiency by increasing the number of immune cells. *PLoS One*. 2014;9(12):e114934.
8. Xiao L, Chen B, Feng D, Yang T, Li T, Chen J. TLR4 may be involved in the regulation of colonic mucosal microbiota by vitamin A. *Front Microbiol*. 2019;10:268.
9. Chen B, Liu S, Feng D, et al. Vitamin A deficiency in the early-life periods alters a diversity of the colonic mucosal microbiota in rats. *Front Nutr*. 2020;7:580780.
10. Ghosh S, Whitley CS, Haribabu B, Jala VR. Regulation of intestinal barrier function by microbial metabolites. *Cell Mol Gastroenterol Hepatol*. 2021;11(5):1463–1482.
11. Feng D, Chen B, Zeng B, et al. Fecal microbiota from children with vitamin A deficiency impair colonic barrier function in germ-free mice: the possible role of alternative bile acid metabolites. *Nutrition*. 2021;90:111274.
12. Ríos-Covián D, Ruas-Madiedo P, Margolles A, Gueimonde M, de Los Reyes-Gavilán CG, Salazar N. Intestinal short chain fatty acids and their link with diet and human health. *Front Microbiol*. 2016;7:185.
13. Liu P, Wang Y, Yang G, et al. The role of short-chain fatty acids in intestinal barrier function, inflammation, oxidative stress, and colonic carcinogenesis. *Pharmacol Res*. 2021;165:105420.
14. Koh A, De Vadder F, Kovatcheva-Datchary P, Bäckhed F. From dietary fiber to host physiology: short-chain fatty acids as key bacterial metabolites. *Cell*. 2016;165(6):1332–1345.
15. Liu H, Wang J, He T, et al. Butyrate: a double-edged sword for health? *Adv Nutr*. 2018;9(1):21–29.
16. Goto Y, Kiyono H. Epithelial barrier: an interface for the cross-communication between gut flora and immune system. *Immunol Rev*. 2012;245(1):147–163.
17. Wang R, Yang X, Liu J, et al. Gut microbiota regulates acute myeloid leukaemia via alteration of intestinal barrier function mediated by butyrate. *Nat Commun*. 2022;13(1):2522.
18. Dong S, Zhu M, Wang K, et al. Dihydromyricetin improves DSS-induced colitis in mice via modulation of fecal-bacteria-related bile acid metabolism. *Pharmacol Res*. 2021;171:105767.
19. Scott SA, Fu J, Chang PV. Microbial tryptophan metabolites regulate gut barrier function via the aryl hydrocarbon receptor. *Proc Natl Acad Sci U S A*. 2020;117(32):19376–19387.
20. Bernad-Roche M, Bellés A, Grasa L, Casanova-Higes A, Mainar-Jaime RC. Effects of dietary supplementation with protected sodium butyrate on gut microbiota in growing-finishing pigs. *Animals*. 2021;11(7):2137.
21. Liu S, Li E, Sun Z, et al. Altered gut microbiota and short chain fatty acids in Chinese children with autism spectrum disorder. *Sci Rep*. 2019;9(1):287.
22. Koike S, Ueno M, Miura H, et al. Rumen microbiota and its relation to fermentation in lactose-fed calves. *J Dairy Sci*. 2021;104(10):10744–10752.

23. Chen Z, Radjabzadeh D, Chen L, et al. Association of insulin resistance and type 2 diabetes with gut microbial diversity: a microbiome-wide analysis from population studies. *JAMA Netw Open*. 2021;4(7):e2118811.
24. Qin P, Zou Y, Dai Y, Luo G, Zhang X, Xiao L. Characterization a novel butyric acid-producing bacterium *Collinsella aerofaciens* Subsp. *Shenzhenensis* Subsp. Nov. *Microorganisms*. 2019;7(3):78.
25. Fan J, Wang Y, You Y, et al. Fermented ginseng improved alcohol liver injury in association with changes in the gut microbiota of mice. *Food Funct*. 2019;10(9):5566–5573.
26. Marfil-Sánchez A, Seelbinder B, Ni Y, et al. Gut microbiome functionality might be associated with exercise tolerance and recurrence of resected early-stage lung cancer patients. *PLoS One*. 2021;16(11):e0259898.
27. Hughes RL, Horn WH, Finnegan P, et al. Resistant starch type 2 from wheat reduces postprandial glycemic response with concurrent alterations in gut microbiota composition. *Nutrients*. 2021;13(2):645.
28. Yang Q, Liang Q, Balakrishnan B, Belobrajdic DP, Feng QJ, Zhang W. Role of dietary nutrients in the modulation of gut microbiota: a narrative review. *Nutrients*. 2020;12(2):381.
29. Hibberd MC, Wu M, Rodionov DA, et al. The effects of micronutrient deficiencies on bacterial species from the human gut microbiota. *Sci Transl Med*. 2017;9(390):eaal4069.
30. Chang CJ, Lin CS, Lu CC, et al. *Ganoderma lucidum* reduces obesity in mice by modulating the composition of the gut microbiota. *Nat Commun*. 2015;6:7489.
31. Zhou H, Zhao X, Sun L, et al. Gut microbiota profile in patients with type 1 diabetes based on 16S rRNA gene sequencing: a systematic review. *Dis Markers*. 2020;2020:3936247.
32. Li L, Krause L, Somerset S. Associations between micronutrient intakes and gut microbiota in a group of adults with cystic fibrosis. *Clin Nutr*. 2017;36(4):1097–1104.
33. Lee H, Ko G. Antiviral effect of vitamin A on norovirus infection via modulation of the gut microbiome. *Sci Rep*. 2016;6:25835.
34. Amit-Romach E, Uni Z, Cheled S, Berkovich Z, Reifen R. Bacterial population and innate immunity-related genes in rat gastrointestinal tract are altered by vitamin A-deficient diet. *J Nutr Biochem*. 2009;20(1):70–77.
35. Wu Z, Huang S, Li T, et al. Gut microbiota from green tea polyphenol-dosed mice improves intestinal epithelial homeostasis and ameliorates experimental colitis. *Microbiome*. 2021;9(1):184.
36. Li Y, Zhang Y, Wei K, et al. Review: effect of gut microbiota and its metabolite SCFAs on radiation-induced intestinal injury. *Front Cell Infect Microbiol*. 2021;11:577236.
37. Waldecker M, Kautenburger T, Daumann H, Busch C, Schrenk D. Inhibition of histone-deacetylase activity by short-chain fatty acids and some polyphenol metabolites formed in the colon. *J Nutr Biochem*. 2008;19(9):587–593.
38. Song L, Sun Q, Zheng H, et al. *Roseburia hominis* alleviates neuroinflammation via short-chain fatty acids through histone deacetylase inhibition. *Mol Nutr Food Res*. 2022;66(18):e2200164.
39. Noureldein MH, Bitar S, Youssef N, Azar S, Eid AA. Butyrate modulates diabetes-linked gut dysbiosis: epigenetic and mechanistic modifications. *J Mol Endocrinol*. 2020;64(1):29–42.
40. Nakano M, Ohwada K, Shindo Y, et al. Inhibition of HDAC and signal transduction pathways induces tight junctions and promotes differentiation in p63-positive salivary duct adenocarcinoma. *Cancers*. 2022;14(11):2584.
41. Zhao Q, Zhang F, Yu Z, et al. HDAC3 inhibition prevents blood-brain barrier permeability through Nrf2 activation in type 2 diabetes male mice. *J Neuroinflammation*. 2019;16(1):103.
42. Saiz-Gonzalo G, Hanrahan N, Rossini V, et al. Regulation of CEACAM family members by IBD-associated triggers in intestinal epithelial cells, their correlation to inflammation and relevance to IBD pathogenesis. *Front Immunol*. 2021;12:655960.
43. Zöllner J, Ebel JF, Khairnar V, et al. CEACAM1 regulates CD8⁺ T cell immunity and protects from severe pathology during *Citrobacter rodentium* induced colitis. *Gut Microb*. 2020;11(6):1790–1805.
44. Chen L, Chen Z, Baker K, et al. The short isoform of the CEACAM1 receptor in intestinal T cells regulates mucosal immunity and homeostasis via Tfh cell induction. *Immunity*. 2012;37(5):930–946.
45. Jin Y, Lin Y, Lin L, Sun Y, Zheng C. Carcinoembryonic antigen related cellular adhesion molecule 1 alleviates dextran sulfate sodium-induced ulcerative colitis in mice. *Life Sci*. 2016;149:120–128.
46. Phan D, Cheng CJ, Galfione M, et al. Identification of Sp2 as a transcriptional repressor of carcinoembryonic antigen-related cell adhesion molecule 1 in tumorigenesis. *Cancer Res*. 2004;64(9):3072–3078.
47. Jia H, Pallos J, Jacques V, et al. Histone deacetylase (HDAC) inhibitors targeting HDAC3 and HDAC1 ameliorate polyglutamine-elicited phenotypes in model systems of Huntington's disease. *Neurobiol Dis*. 2012;46(2):351–361.